J Geod (2005) 79: 71–81
DOI 10.1007/s00190-005-0444-3

ORIGINAL ARTICLE

X.L. Ding · D.W. Zheng · D.N. Dong · C. Ma · Y.Q. Chen · G.L. Wang

Seasonal and secular positional variations at eight co-located GPS and VLBI stations

Received: 23 September 2002 / Accepted: 23 June 2004 / Published online: 6 June 2005

Abstract Time series of daily position solutions at eight co-located GPS and VLBI stations are used to assess the frequency features in the solutions over various time-scales. This study shows that there are seasonal and inter-annual signals in all three coordinate components of the GPS and VLBI solutions. The power and frequency of the signals vary with time, the station considered and the coordinate components, and between the GPS and VLBI solutions. In general, the magnitudes of the signals in the horizontal coordinate components (latitude and longitude) are weaker than those in the height component. The weighted means of the estimated annual amplitudes from the eight GPS stations are, respectively, 1.0, 0.8 and 3.6 mm for the latitude, longitude and height components, and are, respectively, 1.5, 0.7 and 2.2 mm for the VLBI solutions. The phases of the annual signals estimated from the GPS and VLBI solutions are consistent for most of the co-located stations. The seasonal signals estimated from the VLBI solutions are, in general, more stable than those estimated from the GPS solutions. Fluctuations at inter-annual time-scales are also found in the series. The inter-annual fluctuations are up to ∼5 mm for the latitude and longitude components, and up to ∼10 mm for the height component. The effects of the seasonal and inter-annual variations on the estimated linear rates of movement of the stations are also evaluated.

X.L. Ding (✉) · D.W. Zheng · Y.Q. Chen
Department of Land Surveying and Geo-Informatics The Hong Kong Polytechnic University, Hung Hom, KLN, Hong Kong, China;
Tel.: +85-2-27665965
Fax: +85-2-23302994
E-mail: lsxlding@polyu.edu.hk

D.W. Zheng · G.L. Wang
Center for Astrogeodynamics Research, Shanghai Astronomical Observatory, Chinese Academy of Sciences, Shanghai 200030, China

D.N. Dong
Jet Propulsion Laboratory, California Institute of Technology, 4800 Oak Grove Dr., Pasadena, CA 91109, USA

C. Ma
NASA, Space Geodesy Branch, Goddard Space Flight Center, Code 926, Greenbelt, MD 20771, USA

Keywords GPS · VLBI · Station solution · Seasonal signals · Inter-annual variations

1 Introduction

GPS has become one of the most important observational techniques for the study of, e.g., Earth rotation, tectonic plate motions and crustal deformations (e.g., Lindqwister et al. 1991; Springer et al. 1994; Zheng and Xie 1995; Zumberge et al. 1997; Dong et al. 1998; Altiner 2001; Dietrich et al. 2001; Liu et al. 2001; Miller et al. 2001). The IGS's (International GPS Service) GPS network now has more than 250 permanent tracking stations. The reproducibility of the daily GPS solutions provided by some of the IGS Analysis Centres is within a few cm, and that of the weekly solutions is within ∼1 cm.

When examining data from permanent GPS tracking stations, focus has mainly been on the long-term trends of station movements, although seasonal variations in the coordinate series have recently attracted some attention (Blewitt et al. 2000; MacMillan and Ma 2000; Mangialotti et al. 2001; van Dam et al. 2001; Dong et al. 2002; Zhou et al. 2002; Williams 2003). In particular, Dong et al. (2002) and Zhang et al. (2002) examined some of the potential causes of the seasonal variations.

In this work, we will further study the frequency features in the position solutions based on data from eight co-located GPS and VLBI stations. This study will focus especially on the seasonal to inter-annual frequency bands in the coordinate time-series. The wavelet transform will be used to examine the spectra of the data. The least squares method will be employed to estimate the magnitudes and phases of the seasonal signals. The inter-annual signals in the coordinate time-series will also be assessed. Comparison will be made between the results from the GPS and VLBI data.

2 Datasets used for the study

The eight selected co-located GPS and VLBI stations are all in the Northern Hemisphere, with three located on the North

Table 1 Positions of the eight co-located GPS and VLBI stations and summary of the observations obtained at the stations. ("Numd" is the number of daily site solutions; NOAM is the North American plate, PCFC is the Pacific plate and EURA is the Eurasian plate)

Site code	Lat°	Lon°	Observation period	Numd	Plate
GPS stations					
ALGO	45.9558	281.9286	1991, 1,22–2001, 4,28	3012	NOAM
FAIR	64.9780	212.5008	1991, 1,22–2001, 4,28	2931	NOAM
KOKB	22.1263	200.3351	1991, 1,22–2001, 4,28	2832	PCFC
MATE	40.6491	16.7045	1992, 4,22–2001, 4,26	2562	EURA
NALL	78.9296	11.8651	1991, 1,22–2001, 4,28	2360	EURA
ONSA	57.3953	11.9255	1991, 9,29–2001, 4,28	2710	EURA
SHAO	31.0996	121.2004	1995, 1,20–2001, 4,28	1790	EURA
WEST	42.6133	288.5067	1993, 2,14–2001, 4,28	1924	NOAM
VLBI stations					
ALGOPARK	45.9555	281.9273	1984, 8,24–2001, 5,22	330	NOAM
GILCREEK	64.9784	212.5025	1984, 7, 7–2001, 5,22	1435	NOAM
KOKEE	22.1266	200.3349	1993, 6, 8–2001, 5,22	659	PCFC
MATERA	40.6495	16.7040	1990,10, 4–2001, 4,17	264	EURA
NYALES20	78.9291	11.8697	1994,10, 4–2001, 5,22	278	EURA
ONSALA60	57.3958	11.9264	1980, 7,26–2000,12, 7	384	EURA
SESHAN25	31.0992	121.1997	1988, 4, 9–2000,10, 2	81	EURA
WESTFORD	42.6130	288.5062	1981, 5,13–2001, 5, 1	1064	NOAM

American plate, four on the Eurasian plate, and one on the Pacific plate. The maximum distance between the co-located GPS and VLBI antennas is 114 m. The selected stations have reasonably long (∼5-year) spans of GPS and VLBI observations. The daily coordinate solutions (latitude, longitude and height) of the GPS and VLBI stations are used. Further information on the stations and on the observations obtained from the stations are given in Table 1.

2.1 GPS data and pre-processing

The daily GPS solutions, processed by the GPS Analysis Center at the Jet Propulsion Laboratory (JPL) [http://sideshow.jpl.nasa.gov/mbh/series.html] are adopted. The solutions were obtained with the precise point positioning method and the GIPSY software (Zumberge et al. 1997). The satellite orbits, satellite clocks and Earth rotation parameters used for the daily solutions were estimated with data from 42 globally distributed IGS tracking sites. For point positioning, the estimated coordinates of a site are uncorrelated with those of the other sites if the effects of the common errors in the satellite orbits, satellite clocks and Earth rotation parameters on the estimated coordinates are insignificant. The time-series are therefore processed site by site in this study. The daily solutions provide the site position parameters, the stochastic zenith delay and its gradient, the white noise stochastic receiver clock parameters, and the real-valued carrier-phase ambiguities. The JPL analysis uses a cut off elevation angle of 15°, and consistent data processing strategies and software. In addition, corrections for geophysical effects, such as pole and ocean tide effects, have been applied.

The first step in processing the coordinate data series is to estimate and remove the constant term, the linear drift rate and the offsets in each of the data series. The least squares model used for estimating the parameters is

$$y_t = a + bt + c_b + \varepsilon_t \,, \tag{1}$$

where a and b are the constant terms and linear drift, c_b is the offset and ε_t is the noise.

There are data discontinuities in five of the GPS stations (ALGO, FAIR, MATE, ONSA and WEST) that were identified after correspondence with the JPL Analysis Center and from the site logs at the IGS Central Bureau. The discontinuities were due to reasons such as antenna changes at the GPS sites. The offsets were estimated for the latitude, longitude and height components using least squares fitting of the daily position solutions to a constant, a linear drift rate and an offset for each of the data series. The estimated offsets are 1.5, 8.7 and 6.2 mm for ALGO (data prior to Feburary 16, 1994), −0.5, −0.1 and 21.7 mm for FAIR (data prior to April 16, 1996), −2.1, −1.5 and −39.6 mm for MATE (data between April 15 and July 9, 1996), 3.2, 2.8, and −14.3 mm for ONSA (data prior to January 29, 1999) and −3,0, −10.2 and 2.5 mm for WEST (data between May 22 and June 30, 1997). The daily coordinate series, after the estimated constant terms, linear rates and offsets have been removed, are shown in Fig. 1.

2.2 VLBI data

The daily position solutions of the eight VLBI stations, processed by NASA's Goddard Space Flight Center (GSFC quarterly solution 2001 cnse) are adopted for this work. The Mark III VLBI delay data, acquired between August 1979 and February 2001, were analyzed in the VLBI solutions. The basic models used to calculate the VLBI delays are generally consistent with the 1996 international earth rotation service (IERS) conventions (McCarthy 1996). These include the 1980 International Astronomical Union (IAU) nutation (with daily offsets in longitude and obliquity estimated), solid Earth tides (with zero frequency displacement

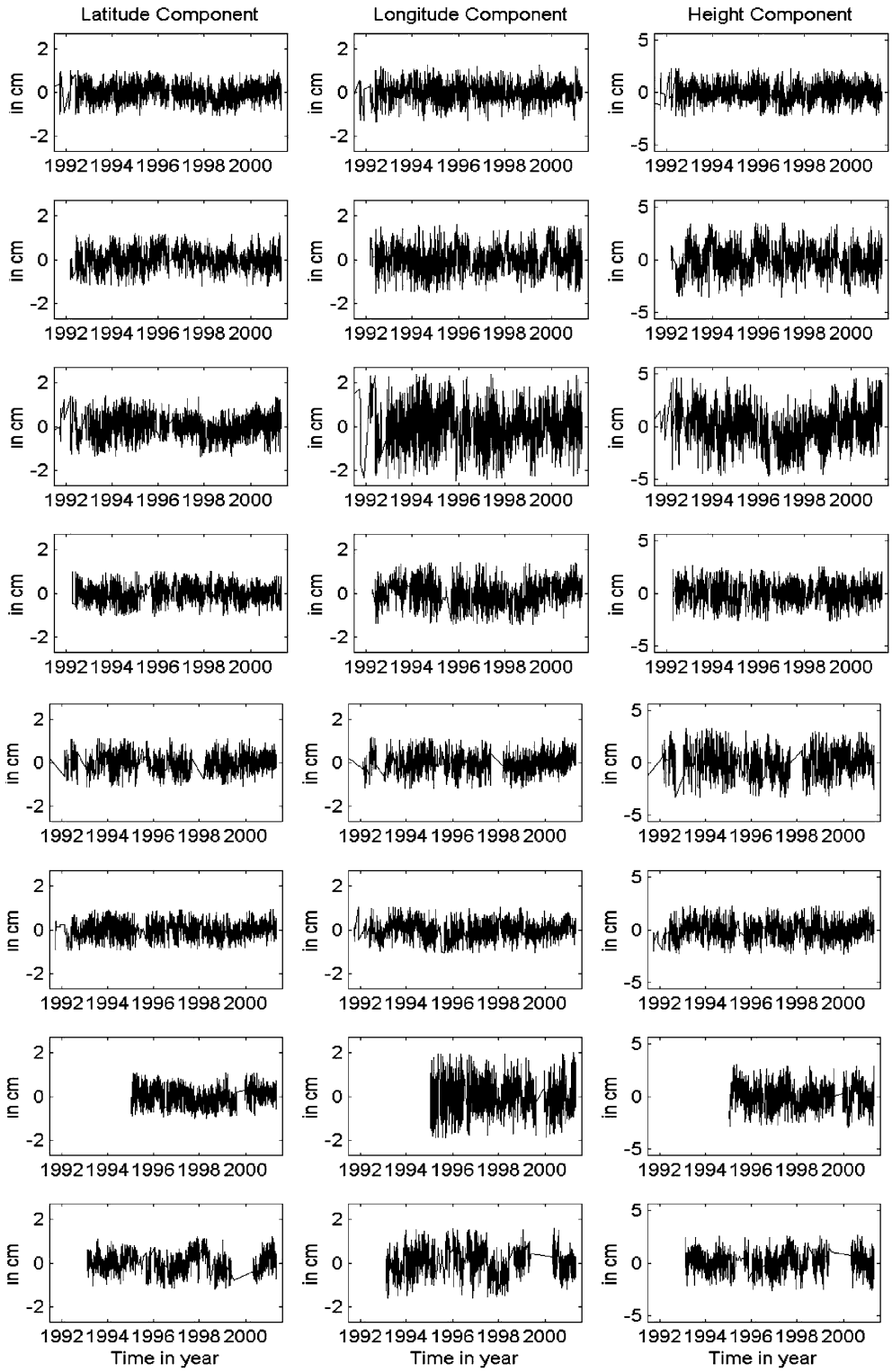

Fig. 1 Time-series of daily position solutions at eight GPS stations. The plots in the first, second and third columns are, respectively, the coordinate variations in the latitude, longitude and height components

but ignoring anelasticity and latitude dependence), pole tide, vertical and horizontal ocean tide loading, and the DE403 solar system ephemeris. The pole position for each observation was interpolated by splining from a one-day input series. In total, 2,534,026 dual-frequency Mark III delays from 2,928 full-day sessions are included in the solution. The solution has

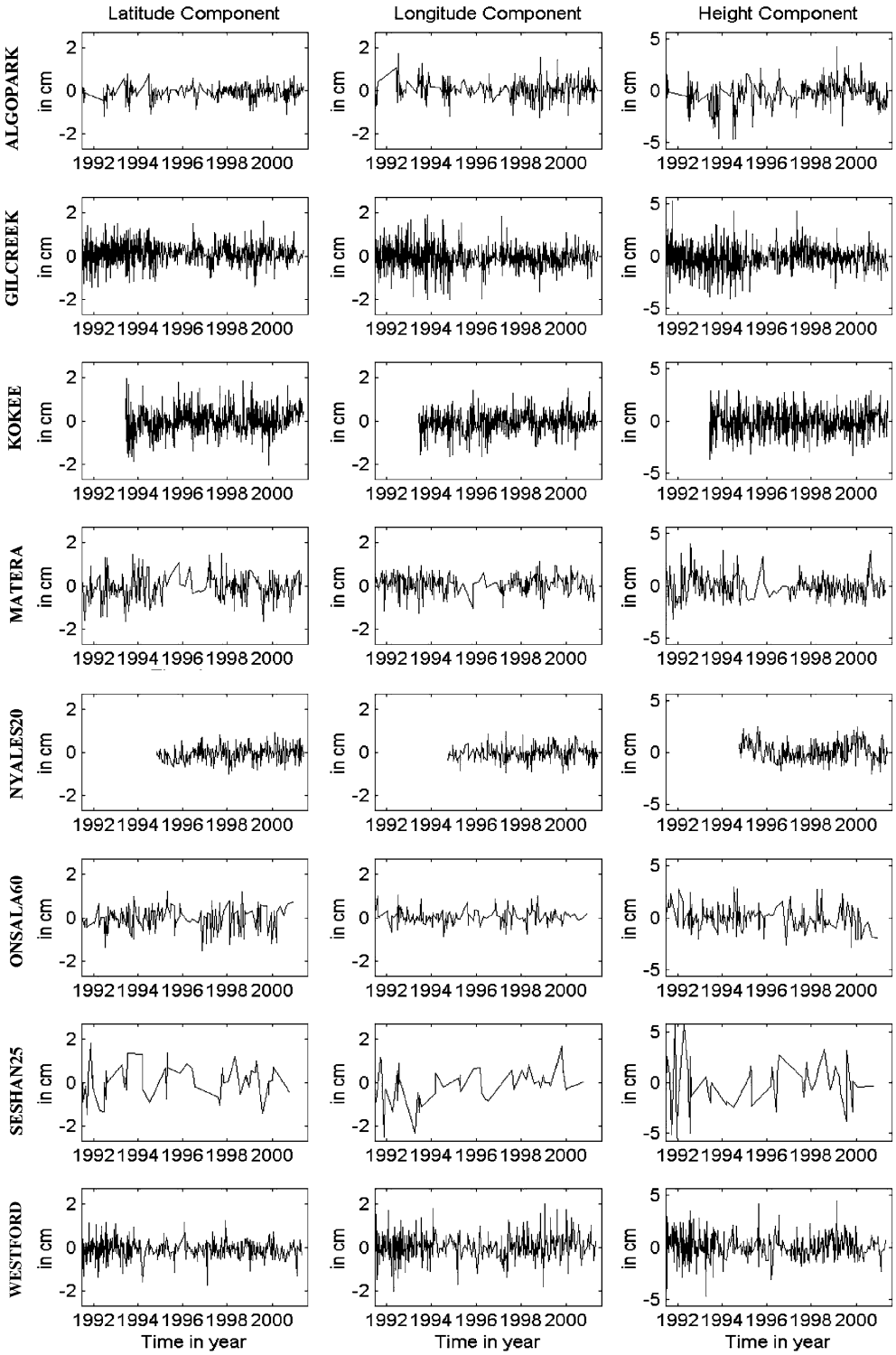

Fig. 2 Time-series of daily position solutions at eight VLBI stations. The plots in the first, second and third columns are, respectively, the coordinate variations in the latitude, longitude and height components

1,304 global parameters and 1,462,917 arc parameters with 1,862,366.4 degrees of freedom. The weighted root mean square (RMS) is calculated from the post-fit delay residuals of the solution is 24.7 ps. The reduced Chi-square statistic is 0.993 when including the constraints for the wet troposphere, gradients, clocks, and earth orientation parameters (EOPs)

in the computation of the degrees of freedom. The reference frame of the VLBI site solutions is tied to the NUVEL-1A NNR model (DeMets et al. 1994).

The daily position solutions of the VLBI stations are shown in Fig. 2. The linear rate has already been removed by GSFC from the daily position solutions before this analysis. It can be seen from Table 1 and by comparing Fig. 1 with Fig. 2 that the amounts of observed daily data points of the VLBI solutions are significantly less than those of the GPS solutions.

3 Spectral analysis of GPS and VLBI solutions

To examine the frequency features in the GPS and VLBI daily solution series, the time-frequency wavelet transform (Chao and Naito 1995; Zheng et al. 2000) is carried out. Given a time series $f(t)$, its wavelet transform is defined as

$$W_\psi(f)(a,b) = \frac{1}{\sqrt{a}} \int_{-\infty}^{\infty} f(t)\psi\left(\frac{t-b}{a}\right) \mathrm{d}t \,, \tag{2}$$

where $\psi(t)$ is the basic wavelet; a is the dilation/compression scale factor that determines the characteristic frequency; and b is the sliding factor in the time domain. In this study, we apply the normalized Morlet wavelet (Morlet et al. 1982) and take the real part of the wavelet transform to characterize the spectrum of each time series. The phases and amplitudes of the signals in the data series are illustrated with the time-varying equal intensity color spectra. The changes of the signals in each of the data series are simultaneously displayed in both the time and frequency domains (referred to as the *a-b* space). The spectral distributions of signals of the different frequencies can also be visualized over the time span.

The wavelet transform is carried out for the GPS and VLBI data series corresponding to four of the eight co-located sites studied (FAIR-GILCREEK, KOKB-KOKEE, NALL-NYALES20 and WEST-WESTFORD). These sites were selected because they have the longest data series among the eight sites studied. Before the wavelet transform is carried out, the data series are first smoothned by taking simple semi-monthly (15.218425 days) mean values. In addition, spline interpolations are used to close gaps in the semi-monthly data series. When carrying out the wavelet transform, the Leap-Step Time Series Analysis (LSTSA) model (Zheng and Luo 1992; Zheng et al. 2000) is used to limit the edge-effects of the wavelet transform. The wavelet spectra thus obtained for the semi-monthly GPS and VLBI time series are shown in Fig. 3.

The three columns in Fig. 3 are, respectively, the spectra of the latitude, longitude and height coordinate series. The rows in Fig. 3 correspond to the four co-located GPS and VLBI stations. The color scheme in Fig. 3 shows the strength of the signals, with the red and blue representing the largest amplitudes (positive and negative corresponding to opposite phases). The post-1997 and post-June 1999 GPS data for stations NALL and WEST, respectively, were not included in the spectral analysis due to large data gaps (seven and eleven months, respectively) in the data series (see Fig. 1); likewise where there are no pre-1995 VLBI data at NYALES20 (see Fig. 2).

It can be seen from the results in Fig. 3 that the spectral structures are quite different among the data series. The strengths and the frequencies of the signals generally vary with time, the station considered and the coordinate components, and are different between the GPS and the VLBI solutions. However, seasonal signals, especially annual ones, can be seen in all the three coordinate components. Comparatively, the signals in the height component are the strongest and the most stable. Some inter-annual signals also exist, although their spectral structures are quite different among the data series. Intra-seasonal signals of higher frequencies can also be seen in the wavelet spectra.

4 Seasonal variations

The amplitudes and phases of the annual and semi-annual signals, and a constant bias were estimated simultaneously from each of the daily solution series with the least squares method of the Householder transform (e.g., Feng et al. 1978). This estimation was based on the following equation

$$S_t = a + \sum_{k=1}^{2} c_k \sin(2\pi t/P_k + \varphi_k) + \varepsilon_t \,, \tag{3}$$

where a is the constant term, and P_k, c_k and $\phi 1_k$ are, respectively, the periods, amplitudes and phases of the annual and semi-annual signals in each of the data series (between 1995.0 and 2001.0). The estimated amplitudes and phases of the annual signals are given in Tables 2, 3 and 4 for the latitude, longitude and height components, respectively. The estimated phases are referred to the epoch of January 1995. The RMS values are calculated from the least squares residuals. The numbers in brackets in the same column are RMS values calculated from the least squares residuals obtained when the seasonal terms in Eq. (3) were not estimated.

It can be seen from the results given in Tables 2, 3 and 4 that the formal uncertainties of the amplitudes and phases estimated from the VLBI data are generally larger than those estimated from the GPS data. It is considered that the main reason for this is that the number of data points in the GPS data series is significantly greater than that of the corresponding VLBI data series (see Table 1). The weighted mean amplitudes of the annual signals of all the GPS stations are 1.0, 0.8, and 3.6 mm, respectively, for the latitude, longitude and height components; the corresponding mean amplitudes of the VLBI stations are 1.5, 0.7, and 2.2 mm. The weight of each of the estimated amplitudes was determined based on its RMS value.

The weighted mean amplitudes of the semi-annual signals were also calculated similarly. The values are generally up to ~1.0 mm for the horizontal components and up to ~2.0 mm for the height component. It is seen from the results in Tables 2, 3 and 4 that the annual and semi-annual signals in

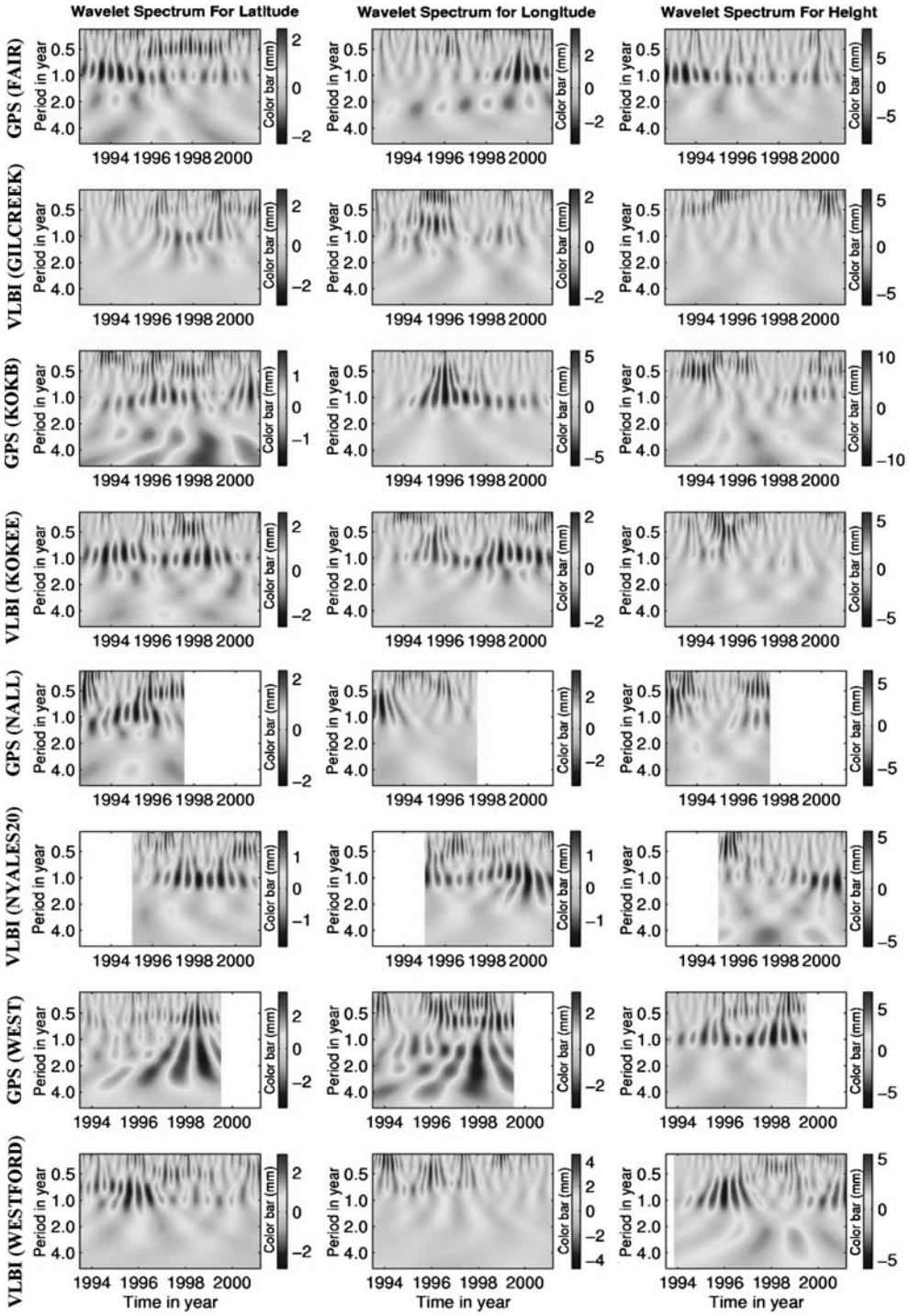

Fig. 3 Time-frequency spectra from the Mortlet wavelet transform of semi-monthly mean site solutions of four co-located GPS and VLBI stations (FAIR-GILCREEK, KOKB-KOKEE, NALL-NYALES20 and WEST-WESTFORD)

the height components of both the GPS and VLBI data series are much stronger than those in the horizontal component.

It can be seen from the results in Table 4 that the GPS and VLBI results are somehow correlated, but the correlation is not very strong. The estimated magnitudes of the annual signals from the GPS data are generally larger than those from the VLBI data. The estimated annual phase values of 5 of the sites are reasonably consistent between the GPS and the VLBI data series, while the estimated phase values of the other three stations are quite different. The mean annual phase difference between the GPS and the VLBI results is 49° and this is reduced to 15° when co-located stations KOKB-KOKEE, NALL-NYALES20 and ONSA-ONSALA60 are excluded.

Table 2 The estimated annual signals (*Am* = amplitude; *Ph* = phase) in the latitude component of the GPS and VLBI position solutions over the time period 1995.0–2001.0. The estimated phases are referred to epoch 1995.0

Stn code	Am (mm)	Ph°	RMS (mm)
GPS Station			
ALGO	1.29 ± 0.10	117.2 ± 4.5	3.13 (3.21)
FAIR	1.52 ± 0.11	79.1 ± 4.1	3.26 (3.55)
KOKB	0.40 ± 0.12	257.5 ± 16.8	3.63 (3.76)
MATE	0.58 ± 0.11	357.4 ± 11.8	3.29 (3.29)
NALL	1.20 ± 0.12	164.0 ± 5.7	3.08 (3.23)
ONSA	0.82 ± 0.11	62.6 ± 7.5	3.08 (3.13)
SHAO	1.36 ± 0.13	46.5 ± 5.4	3.60 (3.72)
WEST	0.77 ± 0.18	69.1 ± 12.8	4.12 (4.44)
VLBI Station			
ALGOPARK	0.43 ± 0.21	131.6 ± 28.3	1.93 (2.20)
GILCREEK	2.22 ± 0.18	185.2 ± 5.2	2.55 (3.11)
KOKEE	1.72 ± 0.24	63.0 ± 7.5	3.33 (3.81)
MATERA	1.34 ± 0.32	352.1 ± 12.8	2.12 (3.39)
NYALES20	1.51 ± 0.23	188.8 ± 9.8	2.41 (2.84)
ONSALA60	1.64 ± 0.66	80.1 ± 22.5	4.02 (4.75)
SESHAN25	5.47 ± 1.34	19.2 ± 15.4	4.71 (9.47)
WESTFORD	1.63 ± 0.20	87.8 ± 7.4	1.97 (2.86)

Table 3 The estimated annual signals (*Am* = amplitude; *Ph* = phase) in the longitude component of the GPS and VLBI position solutions over the time period 1995.0–2001.0. The estimated phases are referred to epoch 1995.0

Stn code	Am (mm)	Ph°	RMS (mm)
GPS Station			
ALGO	0.37 ± 0.11	295.5 ± 16.7	3.26 (3.29)
FAIR	1.38 ± 0.13	84.2 ± 5.4	3.91 (4.17)
KOKB	3.00 ± 0.21	224.6 ± 4.1	6.34 (6.87)
MATE	1.23 ± 0.14	120.2 ± 6.7	4.06 (4.17)
NALL	0.26 ± 0.13	278.0 ± 28.1	3.32 (3.42)
ONSA	0.66 ± 0.10	12.0 ± 9.1	2.97 (3.04)
SHAO	0.98 ± 0.21	224.9 ± 12.2	5.84 (6.10)
WEST	0.69 ± 0.23	25.0 ± 20.2	5.55 (5.58)
VLBI Station			
ALGOPARK	0.59 ± 0.30	13.5 ± 28.6	2.64 (2.95)
GILCREEK	0.47 ± 0.18	67.4 ± 20.7	2.29 (2.79)
KOKEE	1.38 ± 0.19	60.1 ± 7.7	2.68 (3.36)
MATERA	0.41 ± 0.26	201.9 ± 34.5	1.77 (2.48)
NYALES20	1.12 ± 0.21	237.5 ± 10.4	1.91 (2.34)
ONSALA60	0.11 ± 0.28	5.2 ± 148.2	1.62 (2.04)
SESHAN25	2.03 ± 1.52	103.8 ± 38.9	4.78 (5.40)
WESTFORD	1.83 ± 0.31	207.8 ± 9.5	2.78 (3.24)

Table 4 The estimated annual signals (*Am* = amplitude; *Ph* = phase) in the height component of the GPS and VLBI position solutions over the time period 1995.0–2001.0. The estimated phases are referred to 1995.0

Stn code	Am (mm)	Ph°	RMS (mm)
GPS Station			
ALGO	3.37 ± 0.23	194.9 ± 3.9	6.86 (7.46)
FAIR	5.00 ± 0.30	43.3 ± 3.5	9.13 (9.88)
KOKB	3.75 ± 0.42	330.1 ± 6.3	12.12 (12.68)
MATE	1.25 ± 0.28	233.1 ± 12.7	7.80 (7.98)
NALL	3.91 ± 0.34	127.8 ± 5.1	9.16 (10.04)
ONSA	2.44 ± 0.29	131.1 ± 6.7	8.15 (8.40)
SHAO	5.25 ± 0.31	277.9 ± 3.5	8.85 (9.71)
WEST	5.03 ± 0.35	237.6 ± 3.8	8.01 (8.64)
VLBI Station			
ALGOPARK	1.93 ± 0.74	226.0 ± 21.9	6.68 (7.39)
GILCREEK	1.07 ± 0.46	48.8 ± 24.1	6.28 (6.69)
KOKEE	0.87 ± 0.63	79.6 ± 37.8	8.79 (9.34)
MATERA	3.46 ± 0.90	227.2 ± 15.0	6.86 (7.51)
NYALES20	1.98 ± 0.67	24.5 ± 21.3	6.94 (7.66)
ONSALA60	1.99 ± 0.67	24.3 ± 21.3	8.28 (9.31)
SESHAN25	5.12 ± 4.45	264.4 ± 40.0	13.34 (16.90)
WESTFORD	2.30 ± 0.69	218.8 ± 17.0	6.27 (7.45)

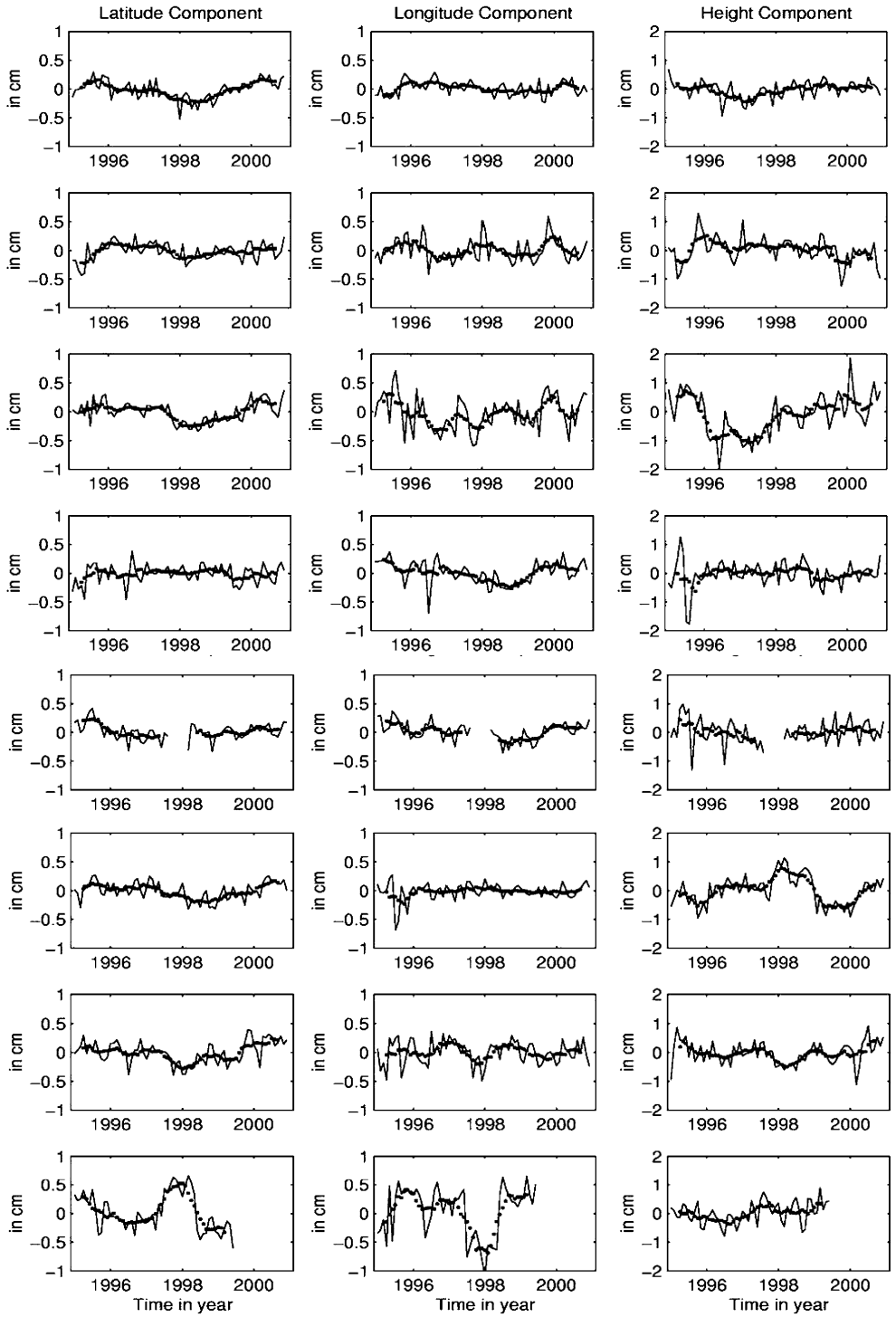

Fig. 4 Inter-annual time-series of the daily GPS solutions over 1995.0–2001.0. The *thin solid lines* are the monthly mean residual series, whilst the *thick dotted lines* are those filtered with seven-point moving averages

The RMS values calculated from the least squares residuals are all reduced when the seasonal terms are included in Eq. (3). The reductions in the RMS values for the VLBI data are generally larger than those for the GPS data, indicating more stable seasonal variations in the VLBI data than in the GPS data.

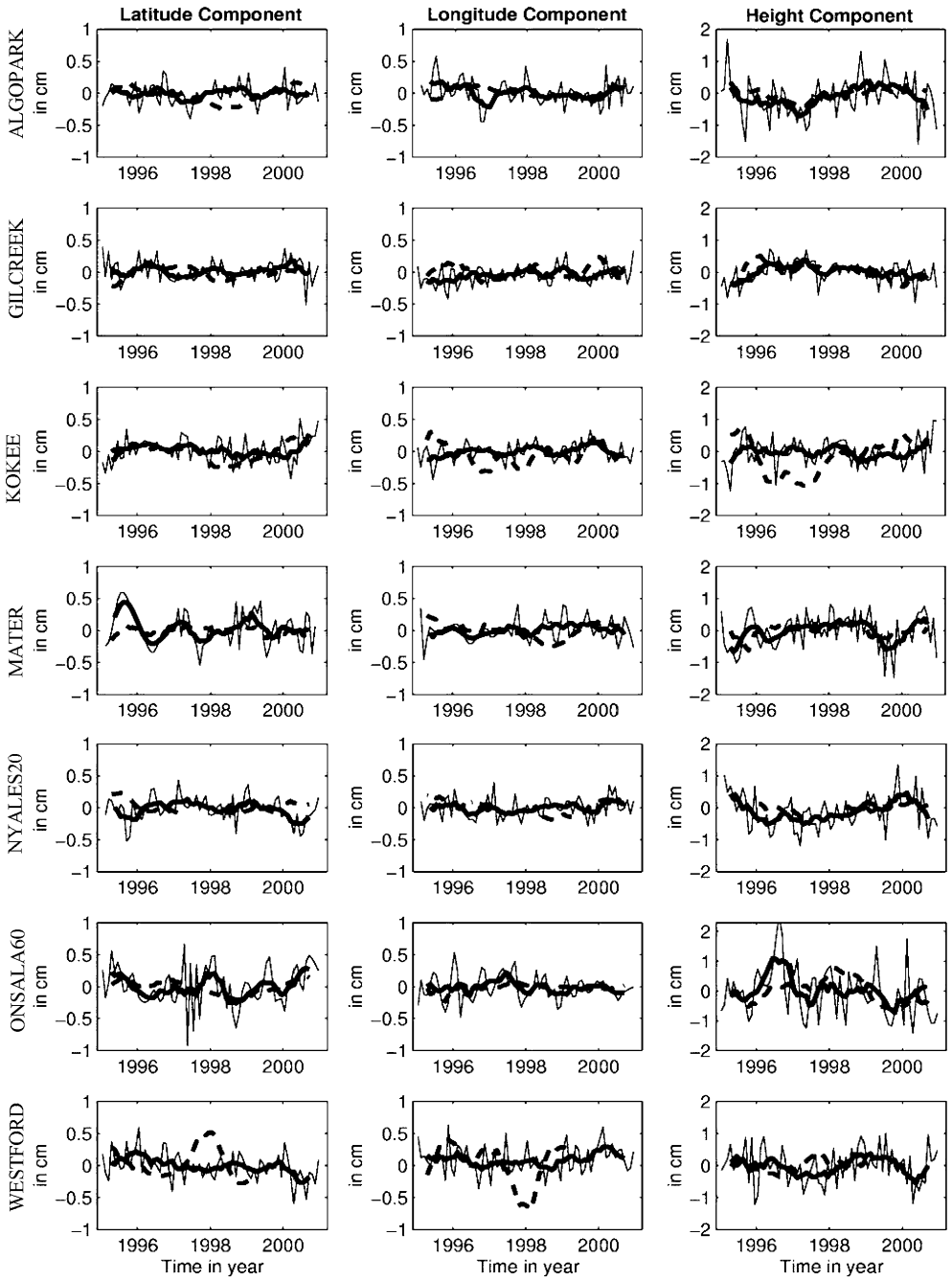

Fig. 5 Inter-annual time-series for the seven VLBI (*thick solid lines*) and GPS (*dashed lines*) stations over 1995.0–2001.0. The *thin lines* are the monthly mean VLBI residual series

5 Inter-annual variations

The monthly mean residuals are calculated by averaging the daily residuals calculated with Eq. (3). The results are plotted in Figs. 4 and 5 as thin solid lines. Besides some residual seasonal and sub-seasonal variations, the monthly mean residuals also show some low-frequency fluctuations. The monthly mean residuals were next filtered with seven-point moving averages to reduce the residual seasonal and sub-seasonal variations. The filtered results are plotted as the thick solid lines in Figs. 4 and 5. The monthly and filtered residuals for the SESHAN25 VLBI station are not given in Fig. 5 as the number of data points is rather small (see Table 1 and Fig. 2).

The filtered monthly residuals in Figs. 4 and 5 show some secular fluctuations on the inter-annual time scale; although it is considered that the data series are too short to fully reflect the true inter-annual variations. Nevertheless, some

Table 5 The estimated linear rates of station movement from daily GPS solutions between 1995.5 and 2000.5, with and without considering the effects of the seasonal and inter-annual variations

Code	Linear rate estimated from raw data			Linear rate estimated from data after seasonal and inter-annual signals have been removed		
	Lat (mm/a)	Lon (mm/a)	h (mm/a)	Lat (mm/a)	Lon (mm/a)	h (mm/a)
ALGO	0.66±0.06	−16.86±0.06	2.80±0.14	0.77±0.06	−16.68±0.06	2.60±0.12
FAIR	−22.30±0.06	−8.13±0.07	−0.86±0.18	−22.12±0.06	−8.13±0.07	−0.05±0.16
KOKB	31.60±0.07	−63.60±0.13	0.18±0.24	31.78±0.06	−63.67±0.11	−1.68±0.19
MATE	18.04±0.07	24.92±0.08	0.26±0.16	18.12±0.07	25.02±0.08	0.27±0.16
NALL	14.68±0.06	10.98±0.07	7.23±0.20	14.70±0.06	11.02±0.06	7.36±0.18
ONSA	14.16±0.06	17.64±0.06	−0.67±0.16	14.36±0.06	17.53±0.06	0.09±0.14
SHAO	−15.28±0.07	32.28±0.12	1.42±0.19	−15.31±0.08	32.25±0.12	1.59±0.18
WEST	4.21±0.12	−16.12±0.15	0.53±0.24	5.02±0.14	−16.33±0.16	−0.82±0.28

Table 6 The RMS values estimated from least squares residuals obtained from the daily GPS solutions between 1995.5 and 2000.5, with and without including the seasonal and inter-annual terms in the least squares regression

Code	RMS when seasonal and "inter-annual" terms are not included			RMS when seasonal and "inter-annual" terms are included		
	Lat (±mm)	Lon (±mm)	h (±mm)	Lat (±mm)	Lon (±mm)	h (±mm)
ALGO	3.25	3.27	7.63	3.01	3.17	6.90
FAIR	3.45	4.12	9.78	3.07	3.74	8.67
KOKB	3.71	6.91	12.57	3.41	6.05	10.99
MATE	3.35	4.17	8.01	3.29	3.89	7.77
NALL	3.27	3.44	10.56	3.02	3.24	9.08
ONSA	3.19	3.09	8.47	2.99	3.03	7.10
SHAO	3.74	5.90	9.41	3.50	5.61	8.32
WEST	4.53	5.70	8.77	3.47	4.63	7.94

inter-annual fluctuations obviously exist in all the three coordinate components of the GPS and VLBI data series. The magnitudes of these [assumed] signals are up to about 5 mm for the latitude and longitude components over the 5.5-year period. The inter-annual variations in the height component are much stronger and range from ∼2–8 mm and ∼3–11 mm for the GPS and the VLBI data series, respectively.

The filtered monthly residuals of the GPS series are plotted as dashed lines in Fig. 5 for comparison. It is interesting to see that the inter-annual variations in the height component determined from the GPS and VLBI data correlate with each other very well for most of the co-located stations, indicating some actual secular fluctuations of station positions or some common site-specific local effects on the two measurement techniques.

To evaluate the possible effects of seasonal and inter-annual variations, especially the latter, on the estimated long-term trends in the data, we first remove the estimated seasonal and inter-annual variations from the daily GPS solution series, and then estimate the constant term and the linear drift rate from each of the data series thus obtained. The results are given in Tables 5 and 6.

It can be seen from Table 5 that the effects of the seasonal and inter-annual signals on the estimated linear rates are small for the latitude and longitude components. For the height component, however, the effects are obviously significant and they mainly came from the inter-annual fluctuations in the data. Therefore, the inter-annual signals should be considered when estimating the vertical rate of station movements. It is shown in Table 6 that the RMS values calculated from the residuals are reduced after the inter-annual signals are modeled. The mean reductions are 9, 8 and 11%, respectively, for the latitude, longitude and height components of the GPS data.

6 Summary and conclusions

Long-term (∼5 years) time-series of daily GPS and VLBI solutions at eight co-located stations distributed over three different tectonic plates in the Northern Hemisphere have been analyzed to identify and assess apparent seasonal and inter-annual signals. Signals of seasonal and inter-annual frequency bands have been detected in both the GPS and the VLBI data series. The strengths and periods of the signals vary with time, stations and coordinate components, and between the GPS and the VLBI solutions. The signals in the latitude and the longitude components are in general weaker than those in the height component. The weighted means of the estimated annual amplitudes for the GPS stations are, respectively, 1.0, 0.8 and 3.6 mm for the latitude, longitude and height components, and are, respectively, 1.5, 0.7 and 2.2 mm for the VLBI solutions

The majority of the stations show consistent annual phase values in the height component between the GPS and VLBI data. The mean annual phase difference between the GPS and the VLBI data is 49°, whilst it reduces to 15° when stations KOKB-KOKEE, NALL-NYALES20 and ONSA-ONSALA60 are excluded. There are some obviously inter-annual variations in all the data series. The magnitudes of the inter-annual signals are up to ∼5 mm for the latitude and longitude components and up to ∼10 mm for the height component. The

signals in the height component are significant compared to the precision of the data. The inter-annual signals determined from the GPS and VLBI data series correlate to each other well for most of the co-located stations.

Possible unmodeled GPS errors, such as phase center errors, local environmental effects and residual tropospheric delays, may also cause various modes of variations in a station coordinate series. It is therefore, necessary to further extend the research, especially by increasing the length of such data series, to investigate the physical reasons for the seasonal and inter-annual variations in the GPS and VLBI data.

Acknowledgements The authors are grateful to Dr. J.F. Zumberge of JPL for his assistance and useful discussions. The constructive comments made by Prof. Thomas Herring, the Responsible Editor, and by an annoymous reviewer are appreciated. The work was partly supported by the Research Grants Council (RGC) of the Hong Kong Special Administrative Region (Project No.: PolyU5067/00E), the Hong Kong Polytechnic University (Project No.: G-YY42), the National Natural Science Foundation of China and the Chinese Academy of Sciences (Project Nos.: 10133010, 10273018 and KJCX2-SW-T1). The research was partly conducted at the Jet Propulsion Laboratory, California Institute of Technology, under a contract with the National Aeronautics and Space Administration.

References

Altiner Y (2001) The contribution of GPS data to the detection of the Earth's crust deformations illustrated by GPS campaigns in the Adria region. Geophys J Int 145:550–559

Blewitt G, Clarke P, Lavalee D (2000) Spatially coherent oscillations in longitude and latitude linked to seasonal variation in Earth's shape. EOS Trans AGU 81:F332

Chao BF, Naito I (1995) Wavelet analysis provide a new tool for studying Earth rotation. EOS Trans AGU 76:161–165

Dietrich R, Dach R, Engelhardt G, Ihde J, Korth W, Kutterer HJ, Lindner K, Mayer M, Menge F, Miller H, Muller C, Niemeier W, Perlt J, Pohl M, Salbach H, Schenke HW, Schone T, Seeber G, Veit A, Volksen C (2001) ITRF coordinates and plate velocities from repeated GPS campaigns in Antarctica – an analysis based on different individual solutions. J Geodyn 74(11–12):756–766

Dong D, Herring TA, King RW (1998) Estimating regional deformation from a combination of space and terrestrial geodetic data. J Geod 72(4):200–214

Dong D, Fang P, Bock Y, Cheng M, Miyazaki S (2002) Anatomy of apparent seasonal variations from GPS derived site position time series. J Geophys Res 107(B4):ETG9-1-ETG9-16

DeMets C, Gordon RG, Argus DF, Stein S (1994) Effect of recent revisions to the geomagnetic reversal time scale on estimates of current plate motions. Geophys Res Lett 21(20):2191–2194

Feng K, Zhang J, Zhang Y, Yang Z, Chao W (1978) Numerical calculation method. National Defense Industry Press, Beijing, p 311

Lindqwister UJ, Zumberge JF, Webb FH, Blewitt G (1991) Few millimeter precision for base-lines in the California permanent GPS geodetic array. Geophys Res Lett 18(6):1135–1138

Liu JY, Chen YI, Chuo YJ, Tsai HF (2001) Variations of ionospheric total electron content during the Chi-Chi earthquake. Geophys Res Lett 28(7):1383–1386

MacMillan DS, Ma C (2000) Analysis of residual VLBI geodetic time series, EOS Trans AGU 81:F314

van Dam TM, Wahr JM, Milly PCD, Shmakin AB, Blewitt G, Lavallee D, Larson KM (2001) Crustal displacements due to continental water loading. Geophys Res Lett 28:651–654

Mangialotti S, Cazenave A, Soudarin L, Cretaux JF (2001) Annual vertical crustal motions predicted from surface mass redistribution and observed by space geodesy. J Geophys Res 106(B3): 4277–4291

McCarthy DD (ed) (1996) IERS Conventions 1996, IERS Technical Note 21, Observatoire due Paris).
[http://maia.usno.navy.mil/conventions.html]

Miller MM, Johnson DJ, Rubin CM, Dragert H, Wang K, Qamar A, Goldfinger C (2001) GPS-determination of along-strike variation in Cascadia margin kinematics: Implications for relative plate motion, subduction zone coupling, and permanent deformation. Tectonics 20(2):161–176

Morlet J, Arehs G, Fourgeau I, Giard D (1982) Wave propagation and sampling theory. Geophysics 47:203–221

Springer TA, Ambrosius BAC, Noomen R, Herzberger K (1994) Results of the Wegener/GPS-92 Campaign. Geophys Res Lett 21(16):1711–1714

Williams SPD (2003) The effect of coloured noise on the uncertainties of rates estimated from geodetic time series. J Geod 73(9–10):483–494

Zhang F, Dong D, Cheng Z, Cheng M, Huang C (2002) Seasonal vertical crustal motions in China detected by GPS. Chin Sci Bull 47(18):1370–1377

Zheng D, Luo S (1992) Contribution of time series analysis to data processing of astronomical observations in China. Stat Sin 2(2): 605–618

Zheng D, Xie B (1995) High-frequency resolution of Earth orientation parameter measured by GPS. Chin Sci Bull 40(12): 1012–1016

Zheng D, Chao BF, Zhou Y, Yu NH (2000) Improvement of edge effect of the wavelet time-frequency spectrum: application to the length of day series. J Geod 74(2):249–254

Zumberge JF, Heflin MB, Jefferson DC, Watkins MM, Webb FH (1997) Precise point positioning for the efficient and robust analysis of GPS data from large networks. J Geophys Res 102(B3): 5005–5017